Most of these effects would tend to destroy the necessary plane wave conditions and reduce the fringe visibility, and in certain cases actually alter the fringe separation. One approximation that can be made is to assume that all the effects that would destroy the Pendellösung would merely add to a monotonic background similar to that of the Darwin curve from a thick crystal. By trial and error we have combined the convoluted curve of Fig. 7 with a monotonic Darwin curve to get the best agreement with our observations. Fig. 8 gives the curve for a ratio of Darwin to Pendellösung of about 10:1. The solid curve represents the sum of the two functions and the monotonic dashed curve is the tail of a Darwin thick crystal curve. The points are the experimental values. The agreement between observation and the solid curve is quite good.

In addition to the shape of the fringes we also measured the mean fringe separation. To the precision with which this value can be determined, we can safely neglect unity compared to η'^2 in equation (17) and have the simple relation between fringe separation f and thickness d

$$f=\Delta_0/d\,. \qquad (23)$$

In Fig. 9 we give the experimentally observed separations *vs* thickness as well as the relationship predicted by equation (23) with a value of $\Delta_0=25{\cdot}6$ μm calculated from the measured $F(333)$ of 5·9.

The scatter is quite large but the data points lie more or less on a straight line tangential to the theory curve at about 18 μm. The deviation for small thickness could possibly be attributed to bending for which the thinner regions would be most sensitive. The agreement with theory is not too satisfactory, but is probably within the rather large uncertainty of the measurements.

Conclusions

Our experiment has verified the existence of the Pendellösung phenomena in the case of Bragg reflection from the surface of a thin crystal. This type of Pendellösung involves the interference of wave fields on the same branch of the dispersion surface and as such is more within the framework of a plane wave, rather than a spherical wave phenomenon.

We have pointed out that an asymmetrical reflection from a perfect crystal has the effect of increasing the lateral coherence of an X-ray beam. By this we mean that asymmetric reflection can produce a beam whose lateral width for a given angular divergence is several orders of magnitude larger than could be obtained by isolating a bundle of that same divergence from a point source of X-rays. The observation of the Pendellösung fringes is an implicit verification that such enhancement of lateral width does indeed take place.

We wish to thank T. C. Madden of the Bell Telephone Laboratories for providing the silicon wafers and Dr P. Ho of Cornell who programmed the computer calculations.

References

BATTERMAN, B. W. & COLE, H. (1964). *Rev. Modern Phys.* **36**, 681.
BATTERMAN, B. W. & PATEL, J. R. (1966). *Acta Cryst.* **21**, A14. *J. Appl. Phys.* To be published.
BONSE, U. (1964). *Z. Physik*, **177**, 543.
COOPER, M. J. (1965). *Acta Cryst.* **18**, 813.
EWALD, P. P. (1933). *Handb. Physik*, **23**, 291.
HART, M. (1966). *Z. Physik*, **89**, 269.
HATTORI, H., KURIYAMA, H., KATAGAWA, T. & KATO, N. (1965). *J. Phys. Soc. Japan*, **20**, 988.
HILDEBRANDT, G. (1959). *Z. Kristallogr.* **112**, 340.
HILDEBRANDT, G. (1968). To be published.
JAMES, R. W. (1963). *Solid State Physics*, **15**, 132.
KATO, N. & LANG, A. R. (1959). *Acta Cryst.* **12**, 787.
KOHRA, K. (1962). *J. Phys. Soc. Japan*, **17**, 589.
VON LAUE, M. (1941). *Röntgenstrahlinterferenzen*, Leipzig: Akademische Verlagsges.
LEFELD-SOSNOWSKA, M. (1964). *Phys. Stat. Sol.* **7**, 449.
MADDEN, T. C. & GIBSON, W. M. (1964). *IEEE Transact. Nuclear Science* NS11, no. 3, 254.
RENNINGER, M. (1961). *Z. Naturforsch.* **16A**, 1110.
ZACHARIASEN, W. H. (1945). *Theory of X-Ray Diffraction in Crystals*. New York: John Wiley.

Acta Cryst. (1968). A**24**, 157

Reciprocity Theorem in Optics and its Application to X-ray Diffraction Topographs

BY N. KATO
Department of Applied Physics, Faculty of Engineering, Nagoya University, Nagoya, Japan

(*Received* 10 *June* 1967)

The reciprocity theorem is applied to X-ray diffraction topographs. The intensity distribution of a traverse-type topograph is obtained by knowing the integrated intensity of the section-type topograph which would be produced with the same crystal by X-rays emitted from a source located virtually at the point concerned. This relation holds in general irrespective of the shape, absorption and distortion of the crystal and the polarization of X-rays.

Introduction

This paper describes a relation between two kinds of X-ray diffraction topograph of transmission type; namely section and traverse topographs. They are most fundamental in transmission diffraction topography. The experimental procedures of taking these topographs are described by Lang (1958, 1959) and Kato & Lang

(1959). In a theoretical paper on the Pendellösung phenomena, which were originally predicted by Ewald (1916*a*,*b*; 1917) on the basis of his theory of crystal optics, the present author has shown the following relation for non-absorbing perfect crystals (Kato, 1961*b*). The intensity at a point of the traverse topograph can be given by the spatially integrated intensity of a section topograph which would be obtained with X-rays emitted from a virtual source located at the point concerned. The basic idea was to use the reciprocity in optics although it was not explicitly mentioned in the previous paper.

The reciprocity theorem, which had been established in optics by Lorentz (1905), was first introduced into X-ray diffraction problems by von Laue (1935). His application to the Kossel lines is one of the most elegant in dynamical diffraction theories. The theorem is now applied to the diffraction topographs and it is shown that the above mentioned relation between the two types of topograph does hold generally for crystals of any shape, absorption and distortion, and X-ray polarization*.

The application of the reciprocity theorem

The theorem is described in a clear form in von Laue's (1935) paper as follows, a slight modification in the presentation being made by the present author. When a light source having a direction h_1 of polarization and located at P_1 excites a current $\mathbf{J}^{(1)}_{h_2,P_2}$ at P_2 in a direction h_2, let us assume that a light source of the same strength and of the direction h_2 of polarization, located at P_2, excites a current $\mathbf{J}^{(2)}_{h_1,P_1}$ at P_1, in the direction h_1. In terms of the field vectors and current vectors thus defined, the theorem states that

$$\mathbf{J}^{(1)}_{h_2,P_2}=\mathbf{J}^{(2)}_{h_1,P_1} \tag{1}$$

and no other component of current is excited at P_1, except in the direction h_1.

In Laue's treatment of Kossel lines, the source is located inside the crystal so that the crystal surrounding the source point should be assumed to be non-absorbing. In the present problem, however, since both the source and the observation point are outside the crystal, absorption can be considered. As in Laue's treatment, the currents at the points P_1 and P_2 are made of only the displacement current $(1/4\pi)\partial\mathbf{D}/\partial t$. Since, in addition, a monochromatic oscillating field is concerned, equation (1) is equivalent to the equation

$$\mathbf{D}^{(1)}_{h_2,P_2}=\mathbf{D}^{(2)}_{h_1,P_1}\,. \tag{2}$$

The suffixes have the same meanings as in equation (1). As mentioned by Laue, the optical distance measured from P_1 to P_2 is the same as that measured from P_2 to P_1.

* The author recalls a conversation with Professor S. Takagi on this problem in 1963. He then mentioned a possible proof based on his dynamical theory for distorted crystals (1962) and independently the idea presented here had occurred to the present author.

First we shall consider a real experiment. The shape, absorbing power *etc.* of the crystal are not specified. The X-ray source is assumed to be a source of spherical waves (Kato, 1961*a*) and located at P_1 in vacuum (Fig. 1). The observation point P_2 is a point on a recording photographic plate. Between the source and the observation point, a diaphragm is placed for eliminating the direct beam P_1P_2 which has nothing to do with the crystal diffraction*. Then, the optical paths starting from P_1 and arriving at P_2 are definitely fixed. In general, the paths may be multiple. Since the following arguments can be applied to any case, we shall consider a single path for simplicity.

X-rays emitted within an infinitesimal solid angle will arrive at an infinitesimal unit area normal to the wave vector $\mathbf{K}_2$ at the observation point P_2. The situation in the usual traverse experiments is equivalent to that in the experiment in which the source (as well as the diaphragm, if necessary) is moved with a constant velocity v on a fixed line with the stationary crystal and the stationary plate. The total energy $I^{(t)}$ passing through a unit area of the recording plate at P_2 is given by

$$I^{(t)}=(c/8\pi)\int_0^T|\mathbf{D}^{(1)}(\tau)|^2\Gamma_2(\tau)d\tau\,. \tag{3}$$

Here, T is the period for the source to be moved over a traverse distance S, $\mathbf{D}^{(1)}(\tau)$ is the displacement vector (*i.e.* electric vector) at P_2. $\mathbf{D}^{(1)}$ may be a function of time τ. The factor $\Gamma_2(\tau)$ is the cosine of the angle be-

* We can avoid inserting the diaphragm in the argument. For this purpose we should assume a source of finite size. The arguments become a little complicated but are essentially similar to the present ones.

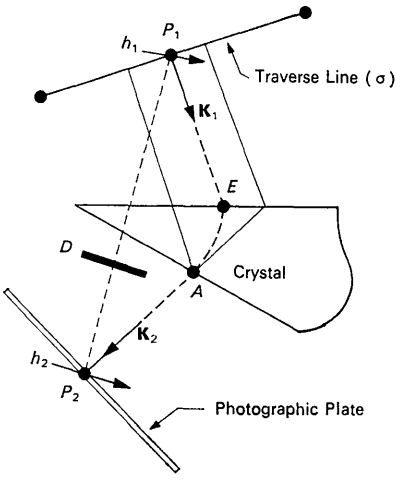

Fig. 1. The real experiment of traverse type with the source at P_1 on the line (σ) and the corresponding virtual experiment of section type with the source at P_2. D: the diaphragm which eliminates the direct beam P_1P_2 or P_2P_1. h_1 and h_2: the direction of polarization. $\mathbf{K}_1$ and $\mathbf{K}_2$: the wave vector. E and A: the entrance and exit points in the real experiment, respectively.

tween $\mathbf{K}_2(\tau)$ and the normal to the plate. In practice, be $\Gamma_2(\tau)$ can be assumed to be a constant, Γ_2.

Next, we shall consider a virtual experiment in which a source of the same strength in the real experiment is put at P_2 during the period T. X-rays, now, are emitted reciprocally from the point P_2. Since the source is fixed, the diffraction (section) topograph on the line σ is unchanged during the period T. Thus, provided that the traverse distance S is wide enough compared with the size of the section topograph produced by the virtual source at P_2, the total energy $E^{(s)}$ received on the distance S is

$$E^{(s)}=(c/8\pi)T\int_0^S|\mathbf{D}^{(2)}(\sigma)|^2\Gamma_1(\sigma)d\sigma\,, \qquad (4)$$

where $\Gamma_1(\sigma)$ is the cosine of the angle of the line σ and the plane normal to the wave vector $\mathbf{K}_1(\sigma)$ of the wave arriving at the position $P_1(\sigma)$. If we consider the section topograph produced by the direct or Bragg-reflected wave, $\Gamma_1(\sigma)$ can be assumed to be a constant $(\Gamma_1)_0$ or $(\Gamma_1)_g$, respectively, with a sufficient accuracy.

In equation (3), the field strength $\mathbf{D}^{(1)}$ is a function of time τ, whereas the strength $\mathbf{D}^{(2)}$ of equation (4) is a function of position σ. The variables are connected through a constant velocity v of traversing as

$$d\sigma=vd\tau\,. \qquad (5)$$

By the reciprocity theorem, we have

$$\mathbf{D}^{(1)}(\tau)=\mathbf{D}^{(2)}(\sigma) \qquad (6)$$

when σ and τ are connected through equation (5). From equations (3), (4), (5) and (6) it is concluded that

$$I^{(t)}_{0,g}=(1/Tv)(\Gamma_2/\Gamma_1)_{0,g}E^{(s)}_{0,g}\,. \qquad (7)$$

The suffixes 0 and g specify the direct and Bragg-reflected waves, respectively. Obviously the factor Tv is the traverse distance S. The geometrical factor $(\Gamma_2/\Gamma_1)_{0,g}$ appears because of the difference of the cross sections of X-ray beams on the line σ and the photographic plate.

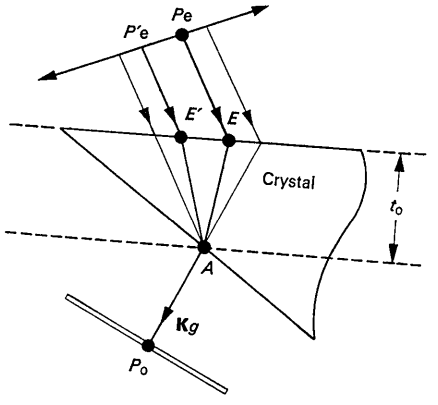

Fig. 2. The conventional procedures for observing the intensity of the traverse topograph. P_e, $P_e'\cdots$: the sources. $E, E'\cdots$: the entrance points. A: the exit point corresponding to the observation point P_o. t_o: the depth of the point A with respect to the entrance surface. $\mathbf{K}_g$: The wave vector of the Bragg-reflected beam.

Discussion and conclusions

For a spherical wave, the integrated intensity (or power ratio) in the section-type experiment can be defined definitely both for the direct and Bragg-reflected waves. It is convenient, therefore, to obtain the intensity distribution of the traverse pattern by the use of the relation (7) derived by the reciprocity theorem. It is important that the theorem can be applied to any kind of materials and geometrical conditions. Although Fig. 1 illustrates a Laue case, the same arguments can be applied also to Bragg cases.

Here, we shall consider traverse topographs of absorbing perfect crystals more in detail, particularly in Laue cases. For obtaining the intensity at a point on the recording plate in the real experiment (*cf.* Fig. 2), we need to know the integrated power ratio of the section topograph for a virtual experiment where the roles of the exit and entrance surfaces are interchanged. The integrated power ratio of the section topograph was obtained in the exact form based on a spherical wave theory (see equation (20) of Kato's (1967) paper). For practical purposes we consider wedge-shaped crystals. Incidentally, strictly speaking the integrated power ratio for wedge-shaped crystals cannot be defined on the basis of the plane wave theory. It should be pointed out here that the geometrical parameters γ_0' and γ_g' appearing in the integrated power ratio, equation (20) mentioned above, must be referred to the exit surface. Further, the distance t_0 used in the formula for specifying the thickness of the crystal must be taken to be the normal distance from the entrance point to the exit surface. Thus, in the formula which gives the intensity of the traverse (real) experiment, the geometrical parameters should be referred to the entrance surface of the real experiment. In addition, the thickness t_0 must be taken to be the normal distance to the entrance surface from the exit point, A, corresponding to the observation point P_0 in the real experiment.

This result justifies the following conventionally accepted considerations in understanding the traverse topographs. In practice, the intensity distribution of the traverse pattern can be assumed to be a projection of the intensity distribution at the exit surface in the direction of the vacuum wave vector, $\mathbf{K}_g$, on the recording plate. The intensity distribution at the exit surface is given by the integrated intensity on the basis of the plane wave theory for a parallel-sided crystal with the same thickness as the depth t_0 of the point A on the exit surface. For absorbing parallel-sided perfect crystals, actually, it is proved that the spherical wave theory and the plane wave theory give the same formula for the integrated intensity (Kato, 1967).

In distorted crystals, also, the integrated intensity cannot be defined by the plane wave theory in the strict sense. Since, it should be obtained on the basis of the

spherical wave theory (*e.g.* Kato, 1964), the relation (7) is particularly useful to know the intensity distribution of traverse topographs.

References

EWALD, P. P. (1916*a*). *Ann. Phys. Lpz.* **49**, 1.
EWALD, P. P. (1916*b*). *Ann. Phys. Lpz.* **49**, 117.
EWALD, P. P. (1917). *Ann. Phys. Lpz.* **54**, 37. (See also *Handbuch der Physik*, **23**, 2, p. 285. Berlin: Springer, 1933).
KATO, N. (1961*a*). *Acta Cryst.* **14**, 526.
KATO, N. (1961*b*). *Acta Cryst.* **14**, 627.
KATO, N. (1964). *J. Phys. Soc. Japan*, **19**, 971.
KATO, N. (1967). *J. Appl. Phys.* In the press.
KATO, N. & LANG, A. R. (1959). *Acta Cryst.* **12**, 787.
LANG, A. R. (1958). *J. Appl. Phys.* **29**, 597.
LANG, A. R. (1959). *Acta Cryst.* **12**, 249.
LAUE, M. VON (1935). *Ann. Phys. Lpz.* **23**, 705.
LORENTZ, H. A. (1905). *Proc. Amsterdam*, **8**, 401.

Acta Cryst. (1968). A**24**, 160

Specimen Motion Effects in Neutron Diffraction*

BY C. G. SHULL, K. R. MORASH AND J. G. ROGERS

Massachusetts Institute of Technology, Cambridge, Massachusetts 02139, *U.S.A.*

(*Received* 16 *June* 1967)

Observations are reported on two effects of specimen motion upon neutron diffraction processes. These include the necessary realignment of a single crystal in maintaining Bragg reflection conditions and the shift in the long wavelength cut-off characteristic of the transmission through a polycrystalline sample. The observations are compared with those to be expected from an analysis of Doppler and velocity compounding effects.

Introduction

Among the three forms of radiation commonly used in crystal diffraction research, namely X-rays, electrons and neutrons, the characteristics of the latter are convenient in demonstrating the dynamical effects of specimen motion on the diffraction process. This arises because the transport velocity of slow neutron radiation is of the same order of magnitude as the laboratory speeds to which crystal specimens can be accelerated. Thus Doppler effects and velocity compounding or aberration effects can be expected to be sizable. A previous study (Shull & Gingrich, 1964) has demonstrated measurable changes in the polycrystalline diffraction pattern with specimen motion and the measured shifts in the position of the Debye–Scherrer reflections were shown to agree with those expected from analysis of the reciprocal lattice construction.

Additional observations on specimen motion effects are supplied in the present report. The present experimental investigations are of two forms, (1) demonstration of the realignment of a single crystal necessitated in maintaining Bragg reflection with crystal motion and (2) illustration of the shift in the long wavelength cut-off edge of the transmission cross section of a polycrystalline specimen. The reported effects are of practical usefulness in neutron technology as will be discussed.

* This research was supported by the National Science Foundation and forms the basis for undergraduate theses submitted by two of us (KRM and JGR) to M.I.T. May 1965.

Single-crystal realignment in Bragg reflection

If a single crystal is set in motion, then it is to be expected that the crystal must be realigned to maintain Bragg reflection of an incident monochromatic neutron beam. This is most conveniently analyzed from the reciprocal lattice construction diagramed in Fig. 1. In this Figure **v** represents the incident neutron velocity, **V** the crystal velocity, and τ the reciprocal lattice vector of the diffracting planes. The diagram illustrates the case where **V** and τ are collinear, implying that the crystal velocity is perpendicular to the Bragg reflecting planes. In the crystal frame of reference, the neutron

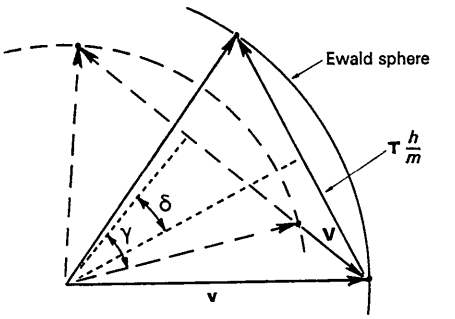

Fig. 1. Reciprocal lattice construction illustrating the reorientation necessary in maintaining Bragg reflection from a moving crystal. The incident neutron velocity is **v**, the crystal velocity is **V** and the reciprocal lattice vector is τ. The dashed line construction corresponds to the moving crystal case with a tilt angle δ of τ to keep the reciprocal lattice point on the Ewald sphere.